Investigation on the electrometric measurement experiment of the artificial thoracic model of pectus excavatum with scoliosis.

Jin-Duo Ye[1], Yong-Wei Hou[1], Wei-Hong Zhong[1]*, Ji-Fu Liu[2], Chun-Qiu Zhang[1]

[1]Tianjin Key Laboratory of the Design and Intelligent Control of the Advanced Mechatronical System, Tianjin University of Technology, Tianjin, PR China

[2]Department of Thoracic Surgery, Military General Hospital of Beijing PLA, Beijing, PR China

Abstract

Introduction: Doctors have to give up surgery for patients with moderate to severe pectus excavatum with scoliosis in clinic. In the experimental study of Nuss procedure, it is not only unable to conduct the experiment *in vivo*, but also cannot get the cadaver of pectus excavatum with scoliosis. Therefore, the calculation method and the result of the finite element model in the numerical simulation still lack of the experimental verification.

Methods: According to the result of numerical simulation, the electrometric measurement, experiment was conducted on an artificial thoracic model which was created by 3D printing technology. By referring to comparison of the experimental and numerical simulation results, the calculation model was modified to improve the accuracy of numerical simulation.

Results: According to the experimental data, the sunken sternum was raised up 40 mm; the Cobb angle of the scoliosis was reduced from 20º to 15.8º, the results of electrometric measurement experiment were basically consistent with those of the numerical simulation and clinic.

Conclusions: This study revealed the strain distribution rules in the view of experiment, and provides a reliable verification method for numerical simulation of the correction of pectus excavatum with scoliosisas well as a reference to optimize the Nuss procedures, to improve the success rate of surgery and to reduce the risk of surgery. With the application of 3D print technology, the limitation of the ethnics and difficulty in producing artificial thoracic model can be overcome.

Introduction

Pectus excavatum with scoliosis is characterized by the deeply sink of sternum and ribs inwards, which presents the fore breast with funnel shape accompanying by distinct scoliosis. There are many reports about pectus excavatum [1-3], but few about pectus excavatum with scoliosis [4]. As the mainstream treatment of pectus excavatum in the current [5,6], the Nuss procedure is an effective technique. However, the operation has to be conducted blindly because its procedure design relies too much on the doctors' experience in clinical and lacks of scientific basis, especially on the patients who have moderate to severe pectus excavatum with scoliosis. Doctors have to give up surgery because blind correction may exacerbate scoliosis in clinic or cause postoperative pain [7]. So it is important to study the intensity and distribution of stress variation on thorax.

The finite element method is an established technique in the field of biomechanics and is used for analysis of various medical situations [8]. Studies have been conducted in recent years to elucidate the Nuss procedure by numerical simulation [7-13], and have obtained some achievements. However, there are still many unsolved problems in the Nuss procedure: the accuracy of the three-dimensional solid model assembly and the finite element model is not sufficient; the given boundary conditions are lack of scientific basis, and the connection of bones is not clear and defined. Therefore, numerical simulation needs to be verified by electrometric measurement experimental. However, restricted by ethics, experiments cannot be conducted *in vivo*.

To solve the above problems, the case of the artificial thoracic model was built based on the rapid prototyping technology-3D printing in this paper, and electrometric measurement experiment was conducted to get the strain distribution. Numerical simulation model was validated and modified on the bases of the experimental results. Guided by the simulation results in clinic, the Nuss procedure was optimized and the risk of the operation reduced.

Methods

Patient

An unsymmetrical pectus excavatum with scoliosis patient (19 y, male) receiving Nuss procedure was included in our study. His concave located on the right of the center and was 40 mm deep in the sagittal plane. His thoracic vertebra bowed 20º to the right, with scoliosis on the same side with the concave. All the operation and medical examinations were conducted in Department of Thoracic Surgery, Military General Hospital of Beijing PLA. The study protocol was approved by the Institutional Review Board of the hospital and written informed consent was obtained from the patient.

Artificial thoracic model

Firstly, 3D model of sternum, ribs and thoracic vertebra was built on the base of CT data with Mimics (Materialise Company), Geomagic studio (Geomagic Company) and Pro/E (PTC) software. Secondly, Rapid Prototyping-3D printer technology was used to create sternum, ribs and thoracic vertebra's model, as shown in Figure 1. Thirdly, in order to keep accuracy of the assembly model, the finite element model of the case was built by ANSYS (ANSYS Company). 12 thoracic vertebras were strung together with aluminium alloy, reinforced with screws 12 pairs of ribs. 2 sternums were connected with ribs by thin metal wire. All the bones were assembled in reference of the finite element model. The final artificial thoracic model is shown in Figures 2 and 3.
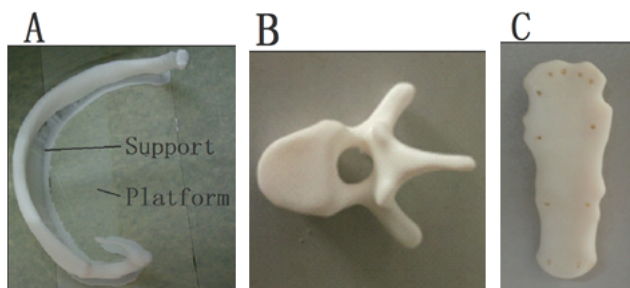

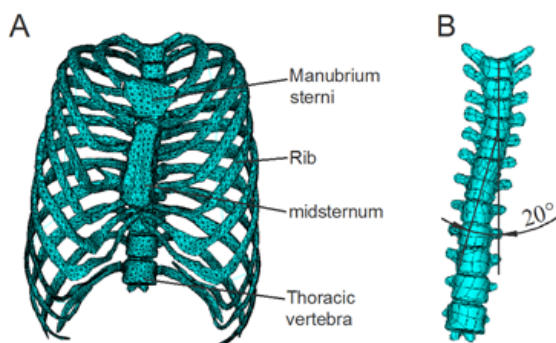***Figure 1.*** *a); The rib after 3D printing b); Thoracic vertebra c) Sternum.*

Figure 2. *a) Finite element model b) Cobb angle of the patient.*
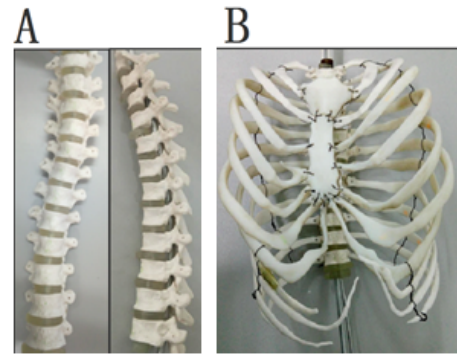

Figure 3. *a) Artificial thoracic vertebra model b) Artificial thoracic skeleton.*

In order to track the strain variation of the artificial thoracic model during electrometric measurement experiment and to reduce the blindness, the paste of the strain gauges were directed by the results of numerical simulation.

According to the numerical simulation results, the largest strain value located on the sternum and their adjacent ribs [14]. Three groups of measurement points around the sternum were selected to observe the strain variation of the artificial thoracic model. A strain gauge was pasted on each measurement point. The first group of strain gauge located on the sternum, having 6 points, as shown in Figure 4a. The second and third groups located on the right (Figure 4b) and left ribs near the sternum (Figure 4c), having 7 points respectively. The fourth group of strain gauge located on the center of right ribs, having 10 points, as shown in Figure 4d.
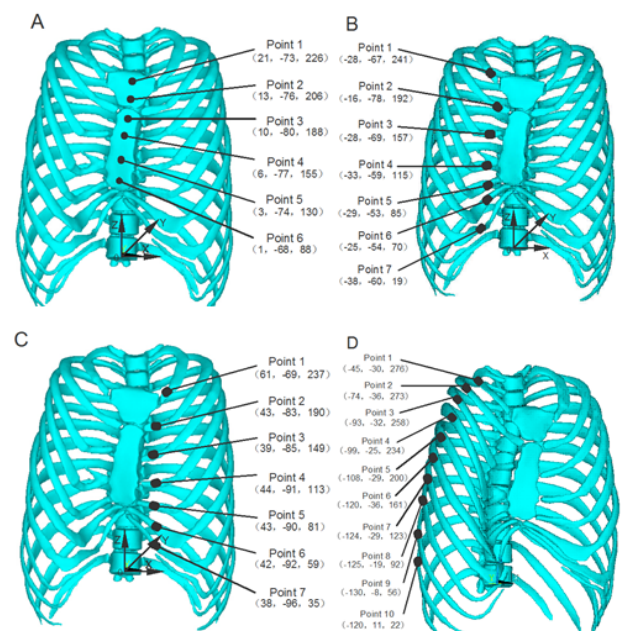

Figure 4. *a) Measuring points on sternum b) Measuring points on right ribs near the sternum c) Measuring points on left ribs near the sternum d) Measuring points on the center right ribs.*

Investigation on the electrometric measurement experiment of the artificial thoracic model of pectus excavatum with scoliosis

Experiment process

The experiment was carried out by the combination of WDW-10 microcomputer control electronic-mechanical universal testing machine (Changchun Kexin Testing Technology Co., LTD) and static/dynamic resistance strain gauge (Donghua Testing Technology Co., LTD). Then the spine model was fixed on the self-made white plaster clamp model, was finally put on WDW-10 electronic universal testing machine. The raising displacement load was applied on the under surface of sternum between the 4th and 5th ribs until the value reached 40 mm. The rising speed was 1 mm/min, and the strain sample interval was 1 sec. The tensile experiment process was repeated 5 times to ensure reliability of the experiment. The interval for each load was 30 minutes to ensure the thorax model to restore to a normal position The model and load device for experiment is shown in Figure 5, as well as the load-displacement curve after 5 repeated load tests is shown in Figure 6.
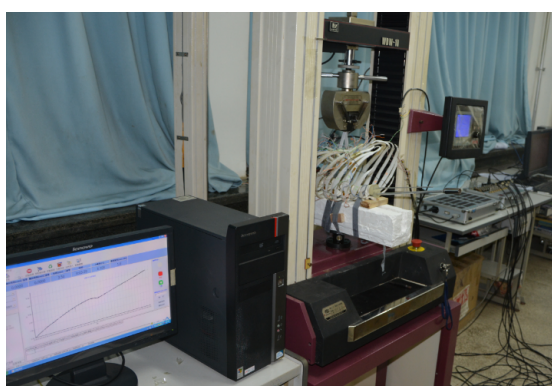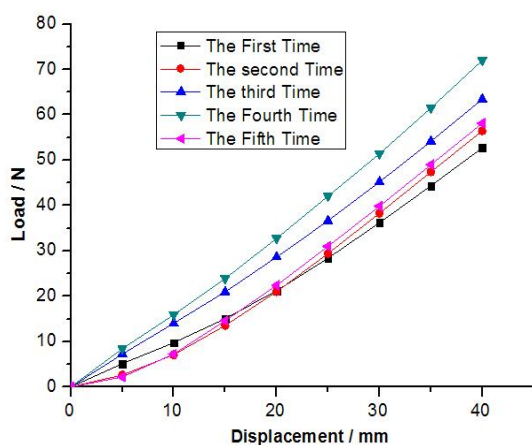

Figure 5. Experiment model and device.

Figure 6. Pre-experiment load-displacement curve.

Results

To ensure the reliability of the experiment, we repeated this experiment three times. The following test data is the mean value of the three experiments. All these results illustrate that four groups of experiment results support the repeatability of data.

Strain distribution of measuring points on sternums

Displacement-strain curve of measuring points on sternums and the result comparison of experiment and numerical simulation are shown in Figures 7 and 8 respectively. Trend of strain at every measuring point is coincident with each other. Before the displacement reaches 15 mm, the strain decline slowly; after the displacement reaches 15 mm, the strains increase rapidly. Because too long costal cartilages result in hysteresis of strain increase while the sternums are lifted. The strains nearby the lifting position show the trend of increase from far to near, which is coincident with the mechanical principles. The maximum strain is 2479.5 µε at measuring point 5, where is the lifting position. Figure 8 indicates that the results of numerical simulation are basically consistent with those of the experiments. Strains of numerical simulation are larger than those of the experiments except that of measuring point 3, which suggests there is great stress concentration at measuring point 3.
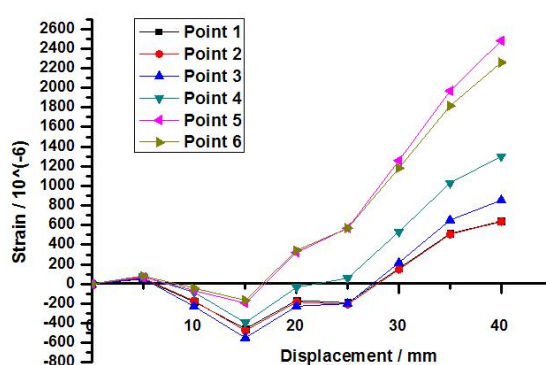

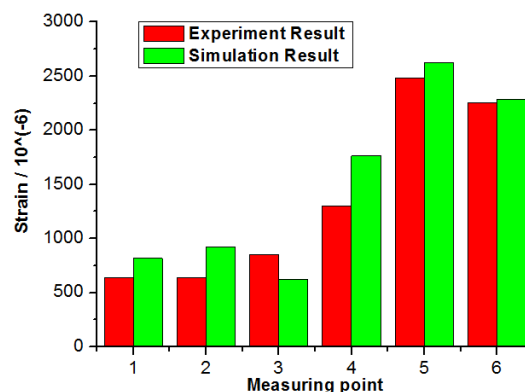*Figure 7. Displacement-strain curves of sternum.*

Figure 8. Experiment vs. simulation strains on sternum.

Strain distribution of measuring points on right ribs near the sternum

Displacement-strain curve of measuring points on right ribs near the sternum and the result comparison of experiment and numerical simulation are shown in Figures 9 and 10 respectively. All measuring points undergo tensile strains, which enlarge rapidly as the displacement increase. The maximum strain is 9467 µε at measuring point 6, on which the deformation is the largest while the sternum is lifting.

Figure 10 indicates that the results of numerical simulation are basically consistent with those of the experiments. Strains of numerical simulation are larger than those of the experiments except that of measuring point 6. The results of the experiments on measuring point 6 is much larger than that of numerical simulation, which suggests there is great stress concentration at measuring point 6.
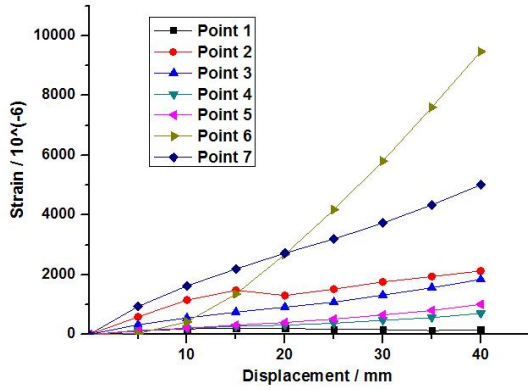

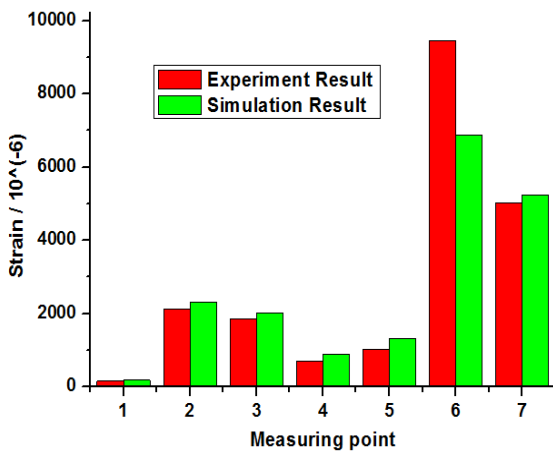*Figure 9. Displacement-strain curves of right ribs.*

Figure 10. Experiment vs. simulation strains on right ribs.

Strain distribution of measuring points on left ribs near the sternum

Displacement-strain curve of measuring points on left ribs near the sternum and the result comparison of experiment and numerical simulation are shown in Figures 11 and 12 respectively. Figure 11 shows that strains enlarge slowly as the displacement increase except measuring point 7. Because the stretches on the left ribs are smaller than those on the right, and the strains vary slowly. The maximum strain is 7799 $\mu\varepsilon$ at measuring point 7, where the costal cartilage is the longest. Figure 12 indicates that the results of numerical simulation are basically consistent with those of the experiments. Strains of numerical simulation are larger than those of the experiments except that of measuring point 7, which suggests there is great stress concentration at measuring point 7.
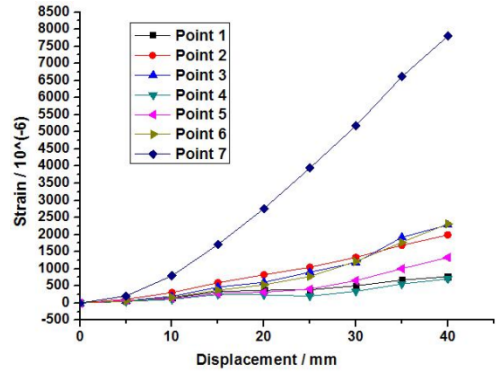

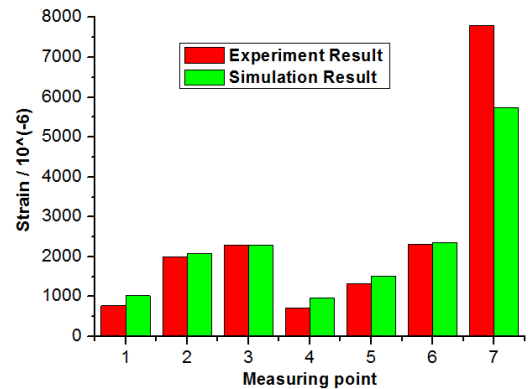*Figure 11. Displacement-strain curves of left ribs.*

Figure 12. Experiment vs. simulation strains on left ribs.

Strain distribution of measuring points on the center of right ribs

Displacement-strain curve of measuring points on the center of right ribs and the result comparison of experiment and numerical simulation are shown in Figures 13 and 14 respectively. Points 8 and 9 undergo tensile strain, the rest points undergo compressional strains. The maximum strain is -1602 $\mu\varepsilon$ at measuring point 3, on which the deformation is the largest while the sternum is lifting.
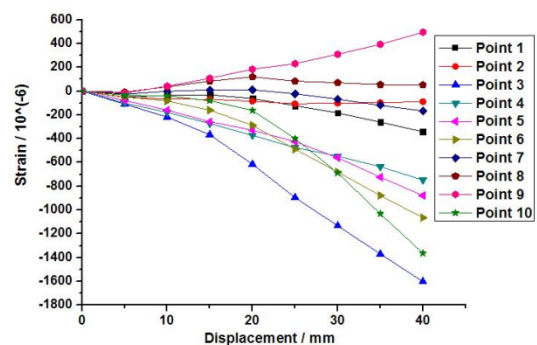

Figure 13. Displacement-strain curves on the center of right ribs.

Figure 14 indicates that the results of numerical simulation are basically consistent with those of the experiments. The results of the experiments on measuring point 3 is much larger than

that of numerical simulation, which suggests there is great stress concentration at measuring point 3.
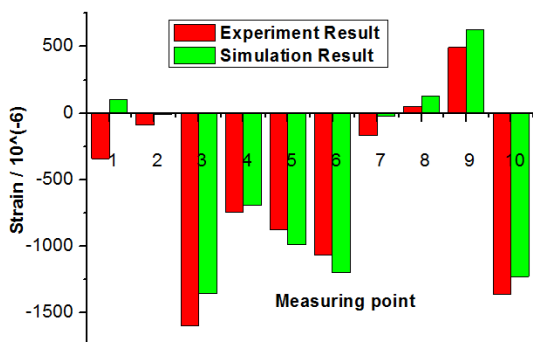

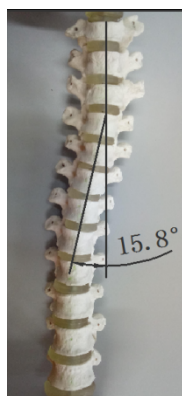***Figure 14.*** *Experiment vs. simulation strains on the center of right ribs.*

Figure 15. *Cobb angle after correction.*

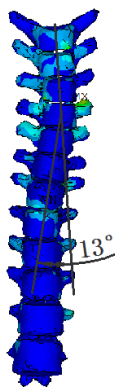***Figure 16.*** *Cobb angle of simulation.*

Scoliosis variation after the correction

Experiment result indicates that the scoliosis is improved after the correction. Cobb angle of the corrected artificial thoracic vertebras is 15.8º, 4.2º smaller than that of uncorrected spine, as shown in Figure 15. Numerical simulation and clinic surgery results of scoliosis are 13º and 15º, and the magnitude of the Cobb angles reduces 7º and 5º respectively compared with that of uncorrected spines, as shown in Figures 15 and 16.

Outcomes of experiment are basically consistent with those of numerical simulation and clinic surgery.

Discussion

Electrometric measurement experiments were conducted on an artificial thoracic model of a patient in this study, and the strain distribution rules of the thoracic skeleton of numerical simulation of the Nuss procedure was evaluated.

The results indicate that strain in artificial thoracic model is not only related to the corrective displacements, but also related to the lifting position. Strains at points near the lifting position are larger than those of others, such as points 5 and 6 in Figure 7. With regard to strain distributions, strain directions on ribs connected with manubrium sterna are positive, strain values are small, such as point 1 in Figures 9 and 11. The strains on ribs connected with mid-sternum are positive and large, especially near the lifting position, such as point 6 in Figure 9, point 7 in Figure 11.

When the Nuss procedure is performed to raise sternal and costal cartilages up, anterior chest ribs are lifted indirectly due to the traction of the lifting force acting on thoracic vertebra from right and left. Unsymmetrical pulling forces are generated on the thoracic vertebras because the pectus excavatum deflects to the right. Concave is deeper on the right beside the sternum, with longer ribs, while milder or no depression on the left, with shorter ribs. Traction from left libs generates larger forces on the thoracic vertebra than those from the right. Hence, the thoracic vertebra on the right are pulled to the left, and the scoliosis is relieved.

To date, several studies on the Nuss procedure have been conducted with numerical simulation [6-14], but no experiments have been done on account of ethnic and shortage of corpse resource. Artificial thoracic model constructed by 3D printing technology is used in electrometric measurement experiment to verify the results of numerical simulation, which provides a new approach in studying mechanical properties of thoracic skeleton. This technique and experimental data may be used to support numerical simulations of correction process, while to provide references to surgeons [11,15,16] in surgery planning.

Nevertheless, because of ethical restrictions and shortage of corpse resource, experiments were performed on a patient's artificial thoracic model. There are many factors affecting the correction process of the patient's artificial thoracic model [17-20]. The human thoracic skeleton is complex because it includes the sternum, thoracic vertebra, ribs, costal cartilage, and vertebral discs, ligaments and intercostal muscles. Artificial thoracic model consists of only the sternum, thoracic vertebra, ribs and vertebral discs, except costal cartilage, ligaments and intercostal muscles which cannot be printed by 3D printing because of the limitations of this technique.

Additionally, there was difference in the materials of vertebral discs between models of the experiment and human thorax, the experimental vertebral discs is harder than that of human

being. The intention of this study aims to provide a preliminary understanding of the relationship between numerical simulation and experimental verification techniques to simulate the Nuss procedure. A large amount of artificial thoracic models will be constructed to perform electrometric measurement experiments in the future to get further investigations.

Conclusions

The strain distribution rules were revealed by the electrometric measurement experiment in this study. The technology of 3D-printing was introduced into electrometric measurement experiment to verify the method and result of numerical simulation of Nuss procedure, the limitation of the ethnics and difficulty in producing artificial thoracic model can be overcome. With the verified numerical simulation of the correction of pectus excavatum with scoliosis, the Nuss procedures planning can be optimized, the success rate of surgery improved, and the risk of surgery reduced.

Conflict of Interest

None of us has financial or personal relationships with people or organizations that could inappropriately influence our work.

Acknowledgements

References

1. Nagasao T, Shimizu Y, Morotomi T. Irregular location of major pectoral muscle can be a causative factor of pectus excavatum. J Med Hypoth 2014; 82: 512-517.

2. Richard E, Readlinger JAW, Robert EK. Optoelectronic plethysmography demonstrates abrogation of regional chest wall motion dysfunction in patients with pectus excavatum after Nuss repair. J Pediatr Surg 2012; 12: 160-164.

3. Willital GH, Saxena AK, Schutze U. Chest-deformities: a proposal for a classification. World J Pediatr 2011; 7: 118-123.

4. Frick SL. Scoliosis in children with anterior chest wall deformities. Chest Surg Clin N Am 2000; 10: 427-436.

5. Nuss D, Kelly RE, Croitoru DP. A 10-year review of a minimally invasive technique for the correction of pectus excavatum. J Pediatr Surg 1998; 33: 545-552.

6. Chang PY, Hsu ZY, Chen DP. Preliminary analysis of the forces on the thoracic cage of patients with pectus excavatum after the Nuss procedure. Clin Biomech 2008; 8: 881-885.

7. Nagasao T, Miyamoto J, Tamaki T. Stress distribution on the thorax after the Nuss procedure for pectus excavatum results in different patterns between adult and child patients. J Thorac Cardiovasc Surg 2007; 134: 1502-1507.

8. Nagasao T, Miyamoto J, Kokaji K. Double-bar application decrease postoperative pain after the Nuss procedure. J Thorac Cardiovasc Surg 2010; 140: 39-44.

9. Nagasao T, Noguchi M, Miyamoto J. Dynamic effects of the Nuss procedure on the spine in asymmetric pectus excavatum. J Thoracic Cardiovasc Surg 2010; 140: 1294-1299.

10. Neves SC, Pinho ACM, Fonseca JC. Finite element analysis of pectus carinatum surgical correction via a minimally invasive approach. J Comp Meth Biomech Biomed Eng 2015; 18: 711-720.

11. Sacco CMG, Gause C, Goldstein SD. Patient satisfaction after minimally invasive repair of pectus excavatum in adults: long-term results of nuss procedure in adults. J Annals Thoracc Surg 2016; 101: 1338-1345.

12. Nagasao T, Hamamoto Y, Tamai M. Scoring of deformed costal cartilages reduces postoperative pain after nuss procedure for pectus excavatum. J Thorac Cardiovasc Surg 2016; 64: 62-69.

13. Zhong W, Ye J, Liu J. Numerical simulation and clinical verification of the minimally invasive repair of pectus excavatum. J Open Biomed Eng 2015; 8: 147-152.

14. Zhao M, Dong P, Ye J. Numerical simulation of minimally invasive correction surgery of pectus excavatum with scoliosis. IEEE Int Conf Mechatr Autom 2014; 1254-1258.

15. Waters P, Welch K, Micheli LJ. Scoliosis in children with pectus excavatum and pectus carinatum. J Pediatr Orthop 1989; 9: 551-556.

16. Fibla JJ, Molins L. Minimally invasive treatment of pectus excavatum. J Minerva Chirurgica 2016; 71: 38-45.

17. Chang PY, Zeng Q, Wong KS. Chest wall constriction after the nuss procedure identified from chest radiograph and multislice computed tomography shortly after removal of the bar. J Thorac Cardiovasc Surg 2016; 64: 70-77.

18. Muhly WT , Maxwell LG, Cravero JP. Pain management following the Nuss procedure: a survey of practice and review. J Acta Anaesthesiologica Scandinavica 2014; 58: 1134-1139.

19. Sacco CMG, Goldstein SD, Gause CD. Minimally invasive repair of pectus excavatum: analysing contemporary practice in 50 ACS NSQIP-paediatric institutions. J Pediatr Surg Int 2015; 31: 493-499.

20. Kabbaj R, Burnier M, Kohler R. Minimally invasive repair of pectus excavatum using the Nuss technique in children and adolescents: Indications, outcomes, and limitations. J Orthop Traumatol Surg Res 2014; 100: 625-630.

*Correspondence to

Wei-Hong Zhong

Tianjin Key Laboratory of the Design and Intelligent Control of the Advanced Mechatronical System

Tianjin University of Technology

PR China